Non-absorbing high-efficiency counter for itinerant microwave photons

Bixuan Fan[1], Göran Johansson[2], Joshua Combes[3], G. J. Milburn[†,1] and Thomas M. Stace[*,1]
[1] *Center for Engineered Quantum Systems, School of Mathematics and Physics, The University of Queensland, St Lucia, Queensland 4072, Australia*
[2] *Microtechnology and Nanoscience, Chalmers University of Technology, S-41296, Göteborg, Sweden and*
[3] *Center for Quantum Information and Control, University of New Mexico, Albuquerque, NM 87131-0001, USA.*

Detecting an itinerant microwave photon with high efficiency is an outstanding problem in microwave photonics and its applications. We present a scheme to detect an itinerant microwave photon in a transmission line via the nonlinearity provided by a transmon in a driven microwave resonator. By performing continuous measurements on the output field of the resonator we theoretically achieve an over-unity signal-to-noise (SNR) for a single shot measurement and 84% distinguishability between zero and one microwave photon with a single transmon and 90% distinguishability with two cascaded transmons. We also show how the measurement diminishes coherence in the photon number basis thereby illustrating a fundamental principle of quantum measurement: the higher the measurement efficiency, the greater is the decoherence.

arXiv:1403.4465v1 [quant-ph] 18 Mar 2014

Quantum photodetection has a long history, almost as old as quantum optics beginning with the theoretical work of Glauber [1] and Mandel [2] in the early 1960s. Since then, both the theory and technology of photodetection have advanced dramatically. Conventional photon detectors, such as avalanche photodiode (APD) and photomultiplier tube (PMT), have been widely used in research. However, they destroy the target photon after detection. There are a number of schemes for quantum non-demolition (QND) photon detection [3–8] but typically they require a high-Q cavity for storing the signal mode (single photon to be detected) and a leaky cavity for manipulating and detecting the probe mode. Thus, during one lifetime of the single photon, the probe mode can have many cycles to amplify the detected signal. This type of detection requires repeated measurements and the high-Q cavity limits the bandwidth of photodetection. In the microwave regime the non-absorbing detection of photons is more challenging. Here we propose a scheme for non-absorbing, high efficiency detection of single itinerant microwave photons via the nonlinearity provided by an artificial superconducting atom, a transmon [9].

In our previous work [10], we showed that it is impossible to detect a single microwave photon with signal-to-noise ratio (SNR) greater than unity using a three-level transmon in an open transmission line, due to the saturation effect of transmon response to the probe intensity. In the present work, some important modifications of our previous model are made: we separate the probe and signal tones into two channels, specifically, the probe field is a microwave cavity mode and the signal photon is propagating in a semi-infinite open transmission line [11, 12]. This is experimentally achievable thanks to the excellent anharmonicity of the transmon. In this configuration, the field-atom coupling has significant enhancement compared to the dissipation. The single microwave photon number information is extracted by weak continuous measurements of the probe. For a single transmon, an over-unity SNR (SNR=1.2) has been demonstrated in our simulation, which corresponds to 84% chance to correctly identify a single-photon. To further discriminate a single photon state from the vacuum, two cascaded transmons are utilized and the probability to correctly identify the single photon increases to 90% . An important feature of our model is that, unlike most QND photon detection proposals, the target single microwave photon in our model is an itinerant photon pulse, offering the chance of detecting relatively wide-band single microwave photons.

The scheme for single microwave photon detection is shown in Fig. 1. A transmon is embedded at one end of a semi-infinite transmission line, coupling with a target single microwave photon at its lowest transition. Also, it is coupled to a coherently-driven microwave resonator at its second transition, used as a probe tone for discrimination of the target photon state. This unit can be cascaded using circulators to achieve higher detection efficiency; a similar structure has been used in [8]. In the following, the case of a single transmon and two cascaded transmons will be investigated. The detection process includes two parts: generation of nonlinear interaction between the probe field and the target photon (control field); and the Homodyne detection of the probe field.

First, we will discuss the detection process using a single transmon. The Hamiltonian describing the single unit in a rotating frame is given by

$$\begin{aligned} H_s &= \delta_1\hat{\sigma}_{11} + (\delta_1+\delta_2)\hat{\sigma}_{22} \\ &- ig_{12}(\hat{a}\hat{\sigma}_{21} - \hat{a}^\dagger\hat{\sigma}_{12}) - iE(\hat{a}-\hat{a}^\dagger) \end{aligned} \quad (1)$$

where $\hat{a}(\hat{a}^\dagger)$ are the annihilation (creation) operators of the cavity field. g is the coupling strength between the cavity field and the transmon $1 \leftrightarrow 2$ transition and E

[1] * stace@physics.uq.edu.au
[2] † milburn@physics.uq.edu.au

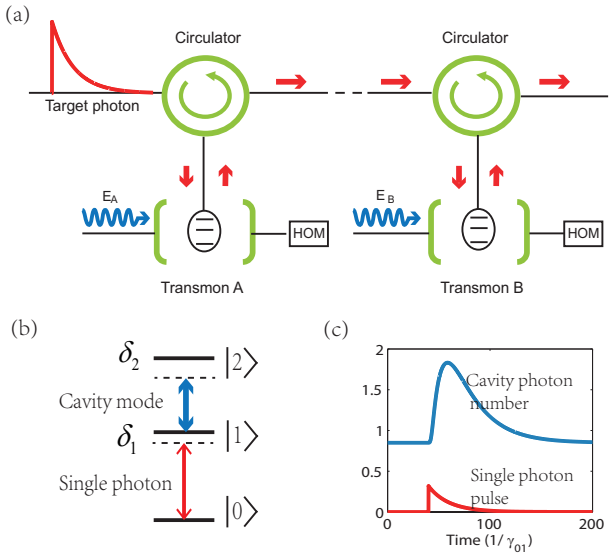

FIG. 1: (Color online) The schematic of single microwave photon counting. (a) A transmon qubit coupled to a microwave cavity is utilized as a nonlinear medium to detect the presence or absence of single microwave photons in a semi-infinite transmission line. When there is no photon in the transmission line, the transmon, prepared in its ground state, cannot be excited to upper energy levels and thus it is transparent to the cavity field; with the presence of the single photon, the cavity field will experience a change due to the interaction with the transmon. A second transmon-cavity unit can be cascaded through a circulator for better distinguishing the single microwave photon state from vacuum state. (b) The energy level structure of the transmon. (c). The response of the cavity field to the incident single photon.

is the driving amplitude. The detunings are defined as $\delta_1 = \omega_{10} - \omega_s$, $\delta_2 = \omega_{21} - \omega_{cav}$.

The system dynamics conditioned continuous measurements can be described by the cascaded, stochastic master equation [13]:

$$d\rho(t) = \mathcal{L}\rho dt + dW(t)\mathcal{H}[e^{-i\phi}\sqrt{\kappa}\hat{a}]\rho \tag{2}$$

where

$$\begin{aligned}\mathcal{L}\rho &= -i[H_s,\rho] + \mathcal{D}[\sqrt{\gamma}_c\hat{c}] + \mathcal{D}[\sqrt{\gamma}_{01}\hat{\sigma}_{01}]\rho \\ &+ \mathcal{D}[\sqrt{\gamma}_{12}\hat{\sigma}_{12}]\rho + \mathcal{D}[\sqrt{\kappa}\hat{a}]\rho \\ &+ \sqrt{\gamma_c\gamma_{01}}([\hat{c}\rho,\hat{\sigma}_{10}] + [\hat{\sigma}_{01},\rho\hat{c}^\dagger])\end{aligned} \tag{3}$$

and the corresponding Homodyne photocurrent is

$$I(t) = \sqrt{\kappa}\left\langle e^{-i\phi}\hat{a} + e^{i\phi}\hat{a}^\dagger\right\rangle + dW(t)/dt \tag{4}$$

where dW is the white noise variable satisfying $E[dW] = 0, E[d^2W] = dt$. $\hat{c}$ is the annihilation operator of the source cavity mode and γ_c is the decay rate of the source cavity, where the target single photon comes from. The phase angle ϕ is selected by tuning the local oscillator phase. The superoperators $\mathcal{D}$ and $\mathcal{H}$ are defined as

$$\begin{aligned}\mathcal{D}[\hat{r}]\rho &= \frac{1}{2}(2\hat{r}\rho\hat{r}^\dagger - \rho\hat{r}^\dagger\hat{r} - \hat{r}^\dagger\hat{r}\rho) \\ \mathcal{H}[\hat{r}]\rho &= \hat{r}\rho + \rho\hat{r}^\dagger - \mathrm{Tr}[\hat{r}\rho + \rho\hat{r}^\dagger]\rho\end{aligned} \tag{5}$$

Prior to arrival of a single photon, the cavity is driven to its steady state with a strong coherent driving, and there is no interaction with the transmon since the transmon is prepared initially in its ground state. At a particular time t_0, a single photon is sent to the system and the transmon will be excited to the middle state, leading to the cavity-transmon interaction and thus producing a change in the cavity field. Since the single photon only interacts with the system for a finite time, the cavity field moves away from the study state amplitude but in the long tie limit it relaxes back to the steady state. Therefore time dependent Homodyne signals are required to detect the single photon. To quantitatively estimate how well we can determine the input photon state, we perform stochastic simulation using Eq. (2) to generate histograms with respect to the initial vacuum state and initial single photon state. If these two histograms are well resolved, then the presence of the single photon can be detected with confidence. The effective signal, $S_{1,0}$, is defined as the integrated Homodyne currents over the interaction time, which is also called Box car filter, $S_{1,0} = \int_{t_0}^{T} I(t)_{1,0}dt$. For Gaussian distributed signals, the SNR can be calculated from the standard formulae $SNR = \frac{\bar{S}_1 - \bar{S}_0}{\sqrt{Var(S_1)+Var(S_0)}}$, with $0, 1$ for the presence/absence of the single photon. We have also used a better linear filter, the response function filter, and the filtered Homodyne signal is:

$$S_f = \int_{t_0}^{T} I(t)h(t)dt \tag{6}$$

where the response function $h(t) = I_{uc}(t)$. I_{uc} is the unconditional measurement result, which is the average response of the cavity to the incident photon.

Due to the nonlinear interaction between the probe field and the transmon, histograms of statistics will be non Gaussian. In this situation, the usual SNR is not the best criterion to justify the detection efficiency. Thus, we introduce an alternative measure, called the distinguishability P_c, defined as the probability of correctly reporting the presence of the single photon given that one was injected. It is defined as $P_c = \frac{1}{2N}(\sum_j (S_1^j > S_{th}) + \sum_j (S_0^j < S_{th}))$ where N is the total trajectory number and S_{th} is the threshold value.

Fig. 2 presents the optimal stochastic simulation results of single microwave photon detection using a single transmon. Left axis is for the histograms of integrated Homodyne currents with the presence and absence of the single microwave photon and the right axis is for the distinguishability P_c between the two possible photon states. The SNR is about 1.2 calculated from the statistics and the distinguishability is about 84%. A significant improvement has been made compared to the configuration used in [10], in which case the SNR is 0.47. If the linear filter is replaced by some nonlinear filters, like hypothesis testing [14, 15] , better detection performance

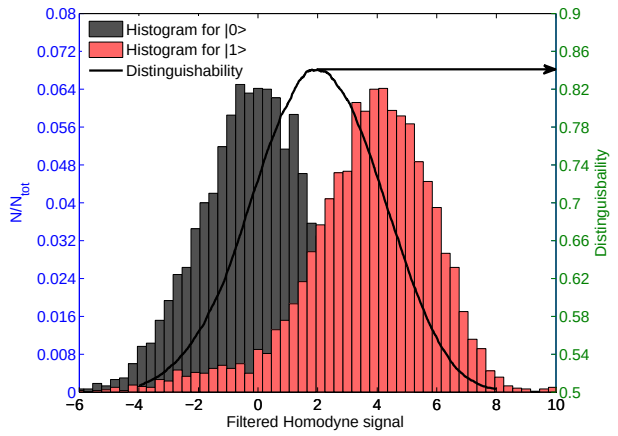

FIG. 2: (Color online) The histograms of filtered Homodyne signal for the presence/absence of the control photon and the corresponding distinguishability. The black curve plots the distinguishability versus threshold values. The single photon pulse is an exponentially-decayed pulse from a source cavity and the linear filter function is presented is Eq. (6). The parameters are: $\gamma = 1$, $\gamma_{12} = 0.1$, $g = 2.45$, $\delta_1 = -0.8$, $\delta_2 = -18$, $\gamma_c = 0.1$, $E = 0.032$, $\kappa = 0.037$ and $T = 80$.

could be expected.

A good cavity, with a long life time, is chosen to make best use of the single-photon induced transmon excitation. Accordingly, the input photon pulse must be a relatively long pulse, matching the long cavity life time. With a long pulse and a good cavity, during the interaction time of the photon with the system, the intra-cavity field changes dramatically, which is not directly bounded by the transmon population. While in the transmission line case, the change in the probe is the atomic polarization $\langle\hat{\sigma}_{12}\rangle$, which is in principle smaller than $\langle\hat{\sigma}_{11}\rangle$ also smaller than 1. After the main part of the photon leaves the system, the transmon excitation will drop to zero very soon due to the relaxation of the transmon. However, at this stage, the induced cavity field is still around its maximum point and then gradually decays to the steady state. This results in a much larger integrated Homodyne signal over the measurement time, although it does limit the average detection rate of a train of single photons.

As mentioned before, the asymmetry or the distortion from a Gaussian distribution of the histogram for $|1\rangle$ results from the nonlinear interaction. A large detuning $\delta_2 \gg g, \kappa, \gamma$ is chosen, so that the effective interaction Hamiltonian of the probe field and transmon is $H_{eff} = \frac{g^2}{\delta_2}\hat{a}^\dagger\hat{a}\hat{\sigma}_{11}$, which indicates a cross-Kerr type interaction between them. The middle state population $\langle\sigma_{11}\rangle$ is determined by the presence or absence of the single photon, so that the transmon induces a large nonlinearity between the single photon and the cavity field.

Next, to further improve the distinguishability, we cascade another transmon using a circulator in the transmission line, with a separate probe cavity. The first and second transmons are labeled as transmon A and transmon B, respectively. Since our detection process is non-absorbing, the single microwave photon will first pass transmon A and then pass transmon B, resulting in dynamical shifts for both cavity modes. Hence, one photon induced two sets of Homodyne currents, which will give a $\sqrt{2}$ improvement in SNR, in principle.

For reduction of computational resources, we unravel the master equation using a number of stochastic processes, including quantum jump and quantum state diffusion [13, 16]. In our model, there are four stochastic processes, three quantum diffusion processes for two cavity fields and relaxation to the transmission line from transition $1 \leftrightarrow 2$ and one quantum jump process for the single photon pulse. When there is no detection of the target microwave photon, the evolution of the unnormalized system wave function $|\bar{\psi}\rangle$ is governed by

$$\begin{aligned} d|\bar{\psi}(t)\rangle &= dt[-i(H_s + H_{cas}) - \frac{1}{2}(\sum_{j=A,B}\kappa_j\hat{a}_j^\dagger\hat{a}_j \\ &+ \gamma_c\hat{c}^\dagger\hat{c} + J^\dagger\hat{J} + J_2^\dagger\hat{J}_2)]|\bar{\psi}(t)\rangle \end{aligned} \quad (7)$$

where

$$\begin{aligned} H_s &= \sum_{j=A,B}(\delta_{j1}\hat{\sigma}_{11}^j + (\delta_{j1}+\delta_{j2})\hat{\sigma}_{22}^j - ig_j(\hat{a}_j\hat{\sigma}_{21}^j \\ &- \hat{a}_j^\dagger\hat{\sigma}_{12}^j) - iE_j(\hat{a}_j - \hat{a}_j^\dagger) \\ H_{cas} &= -i(\sum_{j=A,B}\sqrt{\gamma_c\gamma_{01}^j}\hat{c}\hat{\sigma}_{10}^j \\ &+ \sqrt{\gamma_{01}^A\gamma_{01}^B}\hat{\sigma}_{01}^A\hat{\sigma}_{01}^B + \sqrt{\gamma_{12}^A\gamma_{12}^B}\hat{\sigma}_{12}^A\hat{\sigma}_{12}^B) + h.c. \end{aligned} \quad (8)$$

where we have defined $J = \sqrt{\gamma_c}\hat{c}^\dagger\hat{c} + \sum_{j=A,B}\sqrt{\gamma_{01}^j}\hat{\sigma}_{01}^j$ and $J_2 = \sum_{j=A,B}\sqrt{\gamma_{12}^j}\hat{\sigma}_{12}^j$

When there is a detection of the control photon, the system state will experience a collapse as

$$|\bar{\psi}\rangle = \hat{J}|\bar{\psi}\rangle \quad (9)$$

For both "no detection" and "detection" cases, the wave function has to be normalized as $|\psi\rangle = |\bar{\psi}\rangle / \sqrt{\langle\bar{\psi}|\bar{\psi}\rangle}$.

After performing 8000 trajectories, the two set of data from transmon A and transmon B are obtained. In Fig. 3 (a), the scatter plot of the two set of Homodyne signals $(S_{A1}, S_{A0}; S_{B1}, S_{B0})$ are presented. The majority of the two data sets are distinct with only a small proportion overlapped. To see the exact proportion of the overlap, we average over the two sets of data, $S_{AB} = (S_A + S_B)/2$. In Fig. 3 (b), the histogram of S_{AB} is shown and the Distinguishability here reaches 90%. The vacuum and single-photon states can be well resolved with only 10% overlap. This is equivalent to using the linear boundary

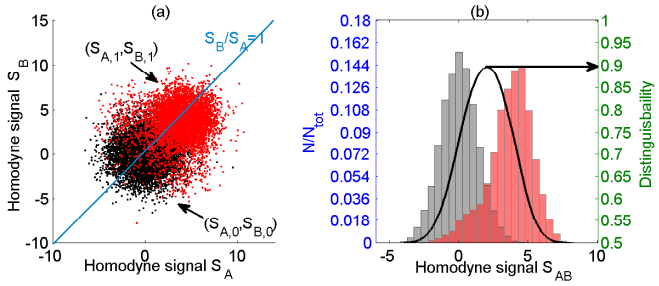

FIG. 3: (Color online) (a). The scatter plot of the filtered Homodyne signals from two probe cavities with the presence/absence of the single photon. (b). The histogram of the sum Homodyne signal S_{AB} and the corresponding distinguishability in the two cascaded transmons case. The parameters are: $\gamma_{01}^A = \gamma_{01}^B = 1$, $\gamma_{12}^A = \gamma_{12}^B = 0.1$, $g_A = g_B = 2.45$, $\delta_{1A} = \delta_{1B} = -0.8$, $\delta_{2A} = \delta_{2B} = -18$, $\gamma_c = 0.1$,$E_A = E_B = 0.032$, $\kappa_A = \kappa_B = 0.037$, and $T = 80$.

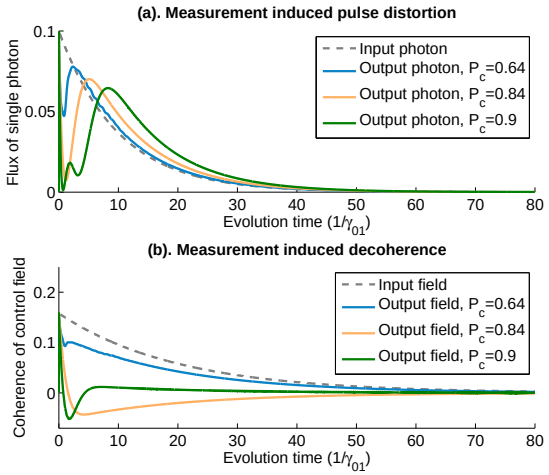

FIG. 4: (Color online) The measurements induced decoherence of the target single microwave photon state. The parameters are the same as in Fig. 3.

of $S_B + S_A = 2S_1$ as a criterion to classify the two sets of data in (a). As expected, the SNR is improved from 1.2 to 1.7 with an approximate $\sqrt{2}$ improvement factor. For ideal Gaussian distribution, $P_c = 0.84$ will be improved to 0.915 when the SNR has a $\sqrt{2}$ improvement. Loss in the distinguishability comes from the non-Gaussian property and also a slight degradation due to the second transmon.

Now, we turn to consider some more general measurement induced effects on the target pulse. According to the general understanding of measurement, good measurement of photon number should cause a decoherence in the number basis. For quantum non-demolition (QND) number measurement, the number information is perfectly preserved since in this type of systems the number operator commutes with the system Hamiltonian so the diagonal elements of the inout state in the umber bassi should be unchanged by measurement. However, physical quantities that do not commute with photon number of the target signal should see added noise. Here we show extra phase noise or pulse distortion caused by QND type measurement, but with number information perfectly preserved. The time evolution for the output single photon flux at different distinguishabilities along with the reference (the flux of the input photon) are ploted in Fig. 4 (a). As the distinguishability between photon states increases, the fidelity between the input and output signal photon decreases, with the total photon number (integrated integrated flux) the same as that of the reference photon. The dip in the photon flux curves comes from the destructive interference between the input field and the transmon polarization. For one transmon, one dip appears on the flux curve and while for two transmons there are two dips. This is because there is a time delay between the excitations of the two transmons induced by the single photon.

Another effect induced by measurements is decoherence. A similar case, qubit measurement induced dephasing, has been discussed in [17, 18]. Suppose $\hat{c}$ is an operator of the field to be measured. In a QND field number measurement, $[\hat{c}^\dagger \hat{c}, H_s] = 0$, while $[\hat{c}, H_s] \neq 0$ and so that the field coherence quantity $\langle \hat{c} \rangle$ is not preserved during the interaction. With a pure Fock state $|1\rangle$ as input, there is no coherence even for the initial state. Therefore, to witness the decoherence effect, we take a superposition state $\frac{1}{\sqrt{2}}(|0\rangle + |1\rangle)$ as the initial state and see how $\langle a(t) \rangle$ evolves in the measurement process. In Fig. 4(b), the time evolution for field coherence at different distinguishability are presented: the gray dashed curve is the reference curve, the coherence of the input state, and the solid curves are the system output curves calculated from the systems with a single transmon and cascaded two transmons. The better is the distinguishability, the faster the loss of the decoherence and when the correct probability P_c at 90%, the field coherence reduces very rapidly to zero. Therefore, while "QND" number measurement ensures that number information of the target system is undisturbed, other physical quantities are changed.

Our scheme is not only suitable for detecting photons at few GHz, it is also applicable to optical photon or other bosonic excitation detection using similar structures. The only disadvantage of our detection scheme is the relative long response time due to the requirement of a good cavity for probe field. Despite this, we believe that our proposal is a promising model for building a non-absorbing high-efficiency counter for itinerant microwave photons.

Bixuan Fan would like to thank Dr. Zhenglu Duan and Dr. Arkady Fedorov for helpful discussions and thank the China Scholarship council and the Center for Engineered Quantum Systems for support. We also acknowledge the

support of the Australian Research council through grant CE110001013

[1] Roy J. Glauber, Phy. Rev. **130**, 2529 (1963).

[2] L. Mandel, E. C. G. Sudarshan and E. Wolf, Proc. Phys. Soc. **84**, 435 (1964).

[3] W. J. Munro, Kae Nemoto, R. G. Beausoleil, and T. P. Spiller Phys. Rev. A **71**, 033819 (2005).

[4] D. F. V. James and P. G. Kwiat, Phys. Rev. Lett. **89**, 183601 (2002).

[5] Sébastien Gleyzes, Stefan Kuhr, Christine Guerlin, Julien Bernu, Samuel Deléglise, Ulrich Busk Hoff, Michel Brune, Jean-Michel Raimond, and Serge Haroche, Nature **446**, 297 (2007).

[6] Ferdinand Helmer, Matteo Mariantoni, Enrique Solano, and Florian Marquardt, Phys. Rev. A **79**, 052115 (2009).

[7] B. R. Johnson, M. D. Reed, A. A. Houck, D. I. Schuster, Lev S. Bishop, E. Ginossar, J. M. Gambetta, L. DiCarlo, L. Frunzio1, S. M. Girvin, and R. J. Schoelkopf, Nature Physics 6, 663 (2010).

[8] S. R. Sathyamoorthy, L. Tornberg, A. F. Kockum, B. Baragiola, J. Combes, C. M. Wilson, T. M. Stace and G. Johansson, arXiv: 1308.2208 (2013).

[9] Jens Koch, Terri M. Yu, Jay Gambetta, A. A. Houck, D. I. Schuster, J. Majer, Alexandre Blais, M. H. Devoret, S. M. Girvin, and R. J. Schoelkopf, Phys. Rev. A **76**, 042319 (2007).

[10] Bixuan Fan, Anton F. Kockum, Joshua Combes, Goran Johansson, Io-chun Hoi, C. M. Wilson, Per Delsing, G. J. Milburn, and Thomas M. Stace, Phy. Rev.Lett. **110**, 053601 (2013).

[11] B. Peropadre, G. Romero, G. Jahansson, C. M. Wilson, E. Salano and J. J. García-Ripoll, Phys. Rev.A **84**, 063834 (2011).

[12] Io-Chun Hoi, Anton F. Kockum, Tauno Palomaki, Thomas M. Stace, Bixuan Fan, Lars Tornberg, Sankar R. Sathyamoorthy, Goran Johansson, Per Delsing, and C. M. Wilson, Phys. Rev. Lett. **111**, 053601 (2013).

[13] H. M. Wiseman and G. J. Milburn, Quantum measurement and control, Cambridge University Press, 2010.

[14] J. Gambetta, W. A. Braff, A. Wallraff, S. M. Girvin and R. J. Schoelkopf, Phys. Rev. A **76**,012325 (2007).

[15] M. Tsang, Phys. Rev. Lett. **108**, 170502 (2012).

[16] M. Moodley and F. Pertuccione, Phys. Rev. A **79**, 042103 (2009).

[17] D. H. Slichter, R. Vijay, S. J. Weber, S. Boutin, M. Boissonneault, J. M. Gambetta, A. Blais, and I. Siddiqi, Phys. Rev. Lett. **109**, 153601 (2012).

[18] M. Brune, E. Hagley, J. Dreyer, X. Maitre, A. Maali, C. Wunderlich, J. M. Raimond and S. Haroche, Phys. Rev. Lett. **77**, 4887 (1996).